

# Tearing instability in relativistic magnetically dominated plasmas

S.S.Komissarov<sup>1</sup>, M.Barkov<sup>1,2</sup>, M.Lyutikov<sup>3</sup>

<sup>1</sup> Department of Applied Mathematics, the University of Leeds, Leeds, LS2 9GT, UK. e-mail: serguei@maths.leeds.ac.uk

<sup>2</sup> Space Research Institute, Moscow, Russia

<sup>3</sup> University of British Columbia, 6224 Agricultural Road, Vancouver, BC, V6T 1Z1, Canada

arXiv:astro-ph/0606375v2 21 Jun 2006

Received/Accepted

## ABSTRACT

Many astrophysical sources of high energy emission, such as black hole magnetospheres, superstrongly magnetized neutron stars (magnetars), and probably relativistic jets in Active Galactic Nuclei and Gamma Ray Bursts involve relativistically magnetically dominated plasma. In such plasma the energy density of magnetic field greatly exceeds the thermal and the rest mass energy density of particles. Therefore the magnetic field is the main reservoir of energy and its dissipation may power the bursting emission from these sources, in close analogy to Solar flares. One of the principal dissipative instabilities that may lead to release of magnetic energy is the tearing instability. In this paper we study, both analytically and numerically, the development of tearing instability in relativistically magnetically-dominated plasma using the framework of resistive magnetodynamics. We confirm and elucidate the previously obtained result on the growth rate of the tearing mode: the shortest growth time is the same as in the case of classical non-relativistic MHD, namely  $\tau = \sqrt{\tau_a \tau_d}$  where  $\tau_a$  is the Alfvén crossing time and  $\tau_d$  is the resistive time of a current layer.

**Key words:** stars:pulsars – black hole physics – MHD – methods:analytical – methods:numerical

## 1 INTRODUCTION

Dissipation of magnetic energy may power high energy emission in a variety of relativistic astrophysical phenomena, e.g. pulsar wind nebulae (Coroniti 1990; Usov 1994; Lyubarsky & Kirk 2001; Kirk & Skjaraasen 2003), jets of active galactic nuclei (Romanova & Lovelace 1992; Jaroschek et al. 2001), gamma-ray bursts (Drenkhahn 2002; Drenkhahn & Spruit H.C. 2002), and magnetars (Thompson & Duncan 1995; Lyutikov 2003).

Perhaps the most clear-cut case for magnetic dissipation is magnetars – neutron stars with superstrong magnetic fields, sometimes in excess of quantum magnetic field  $B_Q = m_e^2 c^3 / \hbar e = 4 \times 10^{13}$  G. (Observationally, magnetars are separated in two classes – Anomalous X-ray Pulsars (AXPs) and the Soft Gamma-ray Repeaters (SGRs) – both showing X-ray flares and quiescent X-ray emission.) A number of evidence suggest that processes that lead to the production of magnetars X-ray flares (and possibly of the persistent emission) are similar to those operating in the Solar corona. The bursting activity of SGRs is strongly intermittent, showing a power law dependence of the number of flares on their energy,  $dN/dE \sim E^\alpha$ , with  $\alpha = 1.66$  and log-normal distribution of waiting times between the flares (Gögüs et al. 1999), both being similar to Solar flares. Giant flares (GFs) be-

low), immense explosions releasing up to  $10^{46}$  ergs in a fraction of a second, provide a number of independent evidence in favour of magnetic dissipation. Two recently observed explosions, from SGR 1900+14 and SGR 1806-20, showed similar behavior leading to and following the GFs: months before the GF X-ray activity increased, spectrum hardened and spindown increased (Mereghetti et al. 2005). In the post-flare period, pulsed fraction and the spin-down rate have significantly decreased and the spectrum softened (Woods et al. 2001; Rea et al. 2005). All these effects are in agreement with the prediction of twisted magnetosphere model (Thompson et al. 2002), with the twist increasing before the GF and decreasing during the GF brought about by reconnection (Lyutikov 2006). Most importantly, observations of the December 27 GF from SGR 1806-20 show very short rise time  $\sim 0.25$  msec (Palmer et al. 2005). Such short rise times are inconsistent with crustal deformations and points to magnetospheric origin of GF (Lyutikov 2006).

In analogy with Solar flares magnetic energy to be dissipated may build-up on long time scales and then be dissipated on very short times scales, possibly as short as Alfvén crossing time. For example, a slow plastic motion of the crust implants a twist (current) in the magnetosphere on a long time scale. At some point a global system of magnetospheric

currents and sheared magnetic fields loses equilibrium and produces a flare. This instability may be dynamical (*e.g.* loss of magnetic equilibrium) and/or resistive (this work).

Though similar in underlying physical process, magnetar and Solar plasmas may differ considerably, since properties of plasma expected in magnetar magnetospheres are very different from the conventional Solar and laboratory plasmas. The principal difference is that magnetar plasma is strongly (relativistically strongly) magnetized. It is convenient to introduce a parameter  $\sigma_m$  (Kennel & Coroniti 1984) as the ratio of the magnetic energy density  $u_B = B^2/8\pi$  to the total plasma energy density (including rest mass!):

$$\sigma_m = \frac{u_B}{u_p} \quad (1)$$

Conventionally, in a non-relativistic Solar and laboratory plasmas, parameter  $\sigma_m$  is small,  $\sigma_m \ll 1$ . On the other hand, in magnetar magnetospheres it is expected that  $\sigma_m$  is very large,

$$\frac{\omega_B R_{NS}}{c} \left( \frac{m_e}{m_p} \right) \sim 10^{13} \leq \sigma_m \leq \frac{\omega_B}{\Omega} \left( \frac{m_e}{m_p} \right) \sim 10^{16} \quad (2)$$

(the upper limit here comes from electron-ion plasma density equal to the Goldreich-Julian density, the lower limit corresponds to plasma density  $\sim B/(R_{NS}c)$  at which point currents drifting with near the speed of light create toroidal magnetic fields of the order of the poloidal). Here  $\omega_B = eB/m_ec$  is cyclotron frequency,  $B$  is magnetic field at the neutron star surface,  $R_{NS}$  is radius of neutron star and  $\Omega$  is rotational frequency.

Large expected value of  $\sigma_m$  (or small  $1/\sigma_m$ ) may be used as an expansion parameter in equations of relativistic magnetohydrodynamics (MHD). The zero order equations, the equations of *magnetodynamics* (MD), describe the dynamics of magnetic field under the action of magnetic pressure and tension (Komissarov 2002). Since to this order the rest mass density and thermodynamic pressure of plasma completely vanish, the only effect plasma has on this dynamics is due to its high conductivity which requires  $\mathbf{E} \cdot \mathbf{B} = 0$  and  $E^2 < B^2$ . Alternatively, one can write the equations of magnetodynamics as Maxwell's equations closed with a suitable Ohm's law that gives the electric current as a function of the electromagnetic field only (Gruzinov 1999). This Ohm's law is derived from the condition of vanishing Lorentz force that explains the alternative name for this system, *force-free degenerate electrodynamics* or simply *force-free electrodynamics*.

The limit  $\sigma_m \rightarrow \infty$  is somewhat reminiscent of the subsonic incompressible hydrodynamic. In this limit the Alfvén four-velocity is  $u_A \sim \sqrt{2\sigma_m} \rightarrow \infty$ , so that both cases are applicable when (four)-velocities are much smaller than the velocity of propagation of disturbances in a medium (Alfvén and sound waves correspondingly). In fact, this analogy turns out to be much deeper: as we discuss in this paper there are deep similarities in governing equations between magnetodynamics a small velocity limit of the conventional magnetohydrodynamics.

In order to address energy dissipation and eventually particle acceleration, one needs to go beyond the ideal approximation. One possible approach is to take into account the dissipation of mostly force-free currents due to plasma

resistivity. Resistivity will result in the decay of currents supporting the magnetic field, which would influence the plasma dynamics. Though plasma resistivity will be of the anomalous type, mediated by plasma turbulence and not by particle-particle collisions, as a first step we assume that plasma resistivity can be represented by macroscopic resistivity parameter  $\eta$ . As another simplification we neglect a possible back reaction of the heated plasma on the global dynamics. This may be justified if the dissipated energy is quickly radiated away.

The principal resistive instability in a conventional, non-relativistic plasma is a so-called tearing mode. It is one of the principle unstable resistive modes, which plays the main role in various TOKAMAK discharges like sawtooth oscillations and major disruptions (Kadomtsev 1975), unsteady reconnection in Solar flares (Shivamoggi 1985; Aschwanden 2002) and Earth magnetotail (Galeev et al. 1978). Qualitatively, the most important property of the tearing mode is that a current layer of thickness  $l$  may dissipate on time scales much shorter than its resistive time scale  $\tau_d \sim l^2/\eta$ . In addition, tearing mode may be an initial stage of the development of the (steady-state) reconnection layers.

Development of the tearing mode in a relativistic, strongly magnetized plasma ( $\sigma_m \gg 1$ ) is the principal topic of this work. Initially, this problem has been considered by Lyutikov (2003), who found that in resistive magnetodynamics the current layers are unstable towards formation of resistive small-scale current sheets, that's to development of tearing mode. He also found that the growth rate of tearing mode is intermediate between the short Alfvén time scale  $\tau_a \sim l/v_a$  (which in a  $\sigma_m \gg 1$  plasma is the light crossing time scale  $\tau_c \sim l/c$ ) and a long resistive time scale  $\tau_d$ :  $\tau \sim (\tau_d \tau_a)^{1/2}$ . Surprisingly, this is exactly the same expression as the one found in the non-relativistic framework of incompressible magnetohydrodynamics. In this paper we uncover the deep underlying reasons for this coincidence. It turns out that slow, resistively-driven evolution of strongly magnetized plasma is described by a system of equations that is very similar to nonrelativistic MHD. In addition to the analytical study we test the theory by means of numerical simulations.

In Section 2 we describe the basic equations of resistive magnetodynamics. In Section 3 we consider the case of slow evolution near equilibrium and show that in this regime the MD equations can be reduced to the system that is very similar to nonrelativistic MHD. Further reduction is possible when the equilibrium is characterized by zero magnetic tension. This is shown in Section 4. The analytic theory of the tearing instability is reviewed in Section 5. Section 6 describes our numerical method and the results of numerical simulations are presented in Section 7.

## 2 BASIC EQUATIONS

In any inertial frame of special relativity the dynamics of electromagnetic field is described by Maxwell's equations. They are the Faraday law

$$\frac{1}{c} \frac{\partial \mathbf{B}}{\partial t} + \nabla \times \mathbf{E} = 0, \quad (3)$$

the magnetic Gauss law

$$\nabla \cdot \mathbf{B} = 0, \quad (4)$$

the Ampere law

$$-\frac{1}{c} \frac{\partial \mathbf{E}}{\partial t} + \nabla \times \mathbf{B} = \frac{4\pi}{c} \mathbf{j}, \quad (5)$$

and the electric Gauss law

$$\nabla \cdot \mathbf{E} = 4\pi\varrho. \quad (6)$$

When these equations are supplemented with the Ohm law, that relates the electric current with the electric field, the system become closed. However, one can also write down additional equations that describe the evolution of the energy and momentum of the electromagnetic field. These additional equations are very useful for physical interpretation of electromagnetic phenomena.

Energy conservation law:

$$\frac{\partial e}{\partial t} + \nabla \cdot \mathbf{S} = -\mathbf{E} \cdot \mathbf{j}, \quad (7)$$

where

$$e = \frac{E^2 + B^2}{8\pi}, \quad (8)$$

is the energy density and

$$\mathbf{S} = \frac{c}{4\pi} \mathbf{E} \times \mathbf{B} \quad (9)$$

is the energy flux density (the Poynting flux).

Momentum conservation law:

$$\frac{\partial \mathbf{p}}{\partial t} + \nabla \cdot \mathbf{T} = -\varrho \mathbf{E} - \frac{1}{c} \mathbf{j} \times \mathbf{B}, \quad (10)$$

where

$$\mathbf{p} = \frac{1}{4\pi c} \mathbf{E} \times \mathbf{B}, \quad (11)$$

is the momentum density and

$$\mathbf{T} = -\frac{1}{4\pi} (\mathbf{E} \otimes \mathbf{E} + \mathbf{B} \otimes \mathbf{B}) + \frac{1}{8\pi} (E^2 + B^2) \mathbf{g} \quad (12)$$

is the Maxwell stress tensor. In the last equation  $\mathbf{g}$  is the metric tensor of Euclidean space,

In strong magnetic field the conductivity across magnetic field can become highly suppressed (when the Larmor frequency becomes much higher than the frequency of particle collisions). Moreover, if the magnetic field is so strong that one can ignore the inertia of plasma particles then the Ohm's law can be written as

$$\mathbf{j} = \varrho \frac{\mathbf{E} \times \mathbf{B}}{B^2} c + \sigma_{\parallel} \mathbf{E}_{\parallel}, \quad (13)$$

where  $E_{\parallel}$  is the component of electric field that is parallel to the magnetic field. Another condition for eq.(13) to hold is  $E < B$ . If this condition is not satisfied the cross-field conductivity has also to be taken into account, e.g. via adding the  $\sigma_{\perp} \mathbf{E}_{\perp}$  term to the right hand side of eq.13. In general, the conductivity  $\sigma_{\parallel}$ , mediated by particle-wave-particle interaction, should depend on the Lorentz factor of plasma through Lorentz transformation of the effective collision rates (Lyutikov 2003). As a simplification, applicable in cases when no strongly relativistic motion *along* the magnetic field lines are expected, here we will assume that  $\sigma_{\parallel}$  is a constant macroscopic parameter.

A characteristic speeds of magnetized plasma is the drift speed of charged particles across magnetic field

$$\mathbf{V} = c \frac{\mathbf{E} \times \mathbf{B}}{B^2}. \quad (14)$$

Note that it appears in the Ohm's law (13) where it describes the non-conductive contribution to the current density.

Given the Ohm law (13) one can write the energy and momentum conservation laws as

$$\frac{\partial e}{\partial t} + \nabla \cdot \mathbf{S} = -\sigma_{\parallel} E_{\parallel}^2, \quad (15)$$

$$\frac{\partial \mathbf{p}}{\partial t} + \nabla \cdot \mathbf{T} = -\varrho \mathbf{E}_{\parallel}, \quad (16)$$

In the limit of infinite conductivity,  $\sigma_{\parallel} \rightarrow \infty$ , the electric current  $j_{\parallel} = \sigma_{\parallel} E_{\parallel}$  must remain finite and this ensures  $\mathbf{E}_{\parallel} \propto \sigma_{\parallel}^{-1} \rightarrow 0$ . In this limit the dynamics of the electromagnetic field can be described by the following closed set of equations (Komissarov 2002)

$$\frac{1}{c} \frac{\partial \mathbf{B}}{\partial t} + \nabla \times \mathbf{E} = 0, \quad (17)$$

$$\nabla \cdot \mathbf{B} = 0, \quad (18)$$

$$\frac{\partial e}{\partial t} + \nabla \cdot \mathbf{S} = 0, \quad (19)$$

$$\frac{\partial \mathbf{p}}{\partial t} + \nabla \cdot \mathbf{T} = 0. \quad (20)$$

In (Komissarov 2002) this system of equations was derived from the system of ideal relativistic MHD in the limit of vanishing rest mass density and pressure of matter. This way of derivation suggests to call this system *magnetodynamics* (MD), the name that is obtained from *magnetohydrodynamics* (MHD) via excluding its *hydro* part. Alternatively, it could be called *force-free degenerate electrodynamics*. This name originates from the early attempts to construct steady-state models of magnetospheres satisfying the degeneracy condition,

$$\mathbf{E} \cdot \mathbf{B} = 0,$$

and the force-free condition,

$$\varrho \mathbf{E} + \frac{1}{c} \mathbf{j} \times \mathbf{B} = 0,$$

e.g. (Thorne & Macdonald 1982). However, it is longer and makes an unwarranted emphasis on the electric component of the electromagnetic field. Indeed, similarly to ideal MHD where the electric field vanishes in the fluid frame, in ideal MD the electric field vanishes in the frame moving with the drift velocity. Thus, the electric component of the field can still be considered as a secondary one that is induced by the motion of magnetized plasma. In fact the electric field vector can be eliminated from the set of dependent variables of equations (17-20) via

$$\mathbf{E} = -\frac{1}{c} \mathbf{V} \times \mathbf{B}, \quad (21)$$

$$e = \frac{B^2}{8\pi} \left( 1 + \frac{V^2}{c^2} \right), \quad (22)$$

$$\mathbf{S} = \frac{B^2}{4\pi} \mathbf{V}, \quad (23)$$

$$\mathbf{p} = \frac{B^2}{4\pi c^2} \mathbf{V}, \quad (24)$$

$$\mathbf{T} = -\frac{1}{4\pi} \left[ \frac{1}{c^2} (\mathbf{V} \times \mathbf{B}) \otimes (\mathbf{V} \times \mathbf{B}) + \mathbf{B} \otimes \mathbf{B} \right] + \quad (25)$$

$$+ \frac{1}{8\pi} B^2 \left( 1 + \frac{V^2}{c^2} \right) \mathbf{g}.$$

Moreover, in the dissipative regime the electromagnetic field can no longer be described as force-free either (see eq.16 ).

### 3 THE QUASI-EQUILIBRIUM APPROXIMATION.

Here we will derive equations that describe slow evolution of strong electromagnetic field near the state of force-free equilibrium. There are two basic characteristic time scales in such problems, the light crossing time scale

$$\tau_c = l/c \quad (26)$$

and the diffusion time scale

$$\tau_d = l^2/\eta, \quad (27)$$

where  $\eta = c^2/4\pi\sigma_{\parallel}$  is the resistivity and  $l$  is the characteristic length scale of the problem. Since in the limit of magnetodynamics the hyperbolic waves (fast and Alfvén waves) propagate with the speed of light then  $\tau_c$  is the typical time of establishing dynamical equilibrium.  $\tau_d$  gives the time scale for the diffusion of magnetic field due to finite resistivity. For systems close to a static equilibrium the characteristic time scale of their global evolution, which we will denote as  $\tau$ , is much larger than  $\tau_c$ . This gives us the small parameter

$$\mu_c = \tau_c/\tau \ll 1. \quad (28)$$

Diffusion is usually only important on small scales where there may exist large gradients of physical quantities. Therefore we will also assume that  $\tau$  is much smaller than  $\tau_d$  and this gives us another small parameter

$$\mu_d = \tau/\tau_d \ll 1. \quad (29)$$

This automatically ensures that the relativistic Lundquist number

$$L_u = \sqrt{2}\tau_d/\tau_c = \sqrt{2}lc/\eta \gg 1 \quad (30)$$

( $\sqrt{2}$  is introduced in order to simplify the expressions of Sec.5.) Moreover, from the Faraday equation one immediately obtains

$$\mathcal{E}/\mathcal{B} = \mu_c \ll 1 \quad (31)$$

where  $\mathcal{E}$  and  $\mathcal{B}$  are the characteristic scales of the electric and the magnetic fields respectively. Thus, the electric field is much weaker than the magnetic field and this results in the drift speed much smaller than the speed of light (see eq.14)

The Ohm law (13) leads to the following dimensionless form of the Ampere equation

$$-\mu_c^2 \frac{\partial \mathbf{E}}{\partial t} + \nabla \times \mathbf{B} = \mu_c^2 \varrho \frac{\mathbf{E} \times \mathbf{B}}{B^2} + \delta_1 \mathbf{E}_{\parallel}, \quad (32)$$

where

$$\delta_1 = (4\pi)^2 L_u \frac{\mathcal{E}_{\parallel}}{\mathcal{B}}. \quad (33)$$

Thus, the Ampere law may be reduced to

$$\nabla \times \mathbf{B} = \frac{4\pi}{c} \sigma_{\parallel} \mathbf{E}_{\parallel} \quad (34)$$

and the characteristic scale for the parallel component of the electric field is

$$\mathcal{E}_{\parallel} = (4\pi)^{-2} L_u^{-1} \mathcal{B} \ll \mathcal{B}. \quad (35)$$

Using this equation and the expression (14) for the drift velocity we can write

$$\mathbf{E} = -\frac{1}{c} \mathbf{V} \times \mathbf{B} + \frac{c}{4\pi\sigma_{\parallel}} \nabla \times \mathbf{B}. \quad (36)$$

Substitution of this result into the Faraday equation leads to the exactly the same advection-diffusion equation for magnetic field as in the nonrelativistic MHD

$$\frac{\partial \mathbf{B}}{\partial t} - \nabla \times (\mathbf{V} \times \mathbf{B}) - \eta \nabla^2 \mathbf{B} = 0. \quad (37)$$

The dimensionless form of the energy equation (15) reads

$$\frac{\partial e}{\partial t} + \nabla \cdot \mathbf{S} = -\delta_2 E_{\parallel}^2, \quad (38)$$

where

$$\delta_2 = \frac{\mu_d}{(4\pi)^2} \ll 1. \quad (39)$$

Thus, the dissipative term may be omitted and the energy equation reduces to its ideal form

$$\frac{\partial e}{\partial t} + \nabla \cdot \mathbf{S} = 0. \quad (40)$$

The dimensionless form of the momentum equation (16) is

$$\mu_c^2 \frac{\partial \mathbf{p}}{\partial t} + \nabla \cdot \mathbf{T} = -\delta_3 \rho E_{\parallel}, \quad (41)$$

where

$$\frac{\delta_3}{\mu_c^2} = \frac{\mu_d}{4\pi} \ll 1. \quad (42)$$

Thus, the resistive term in the momentum equation can also be omitted and we write

$$\frac{\partial \mathbf{p}}{\partial t} + \nabla \cdot \mathbf{T} = 0. \quad (43)$$

Given condition (31) we may write

$$e = \frac{B^2}{8\pi} \quad (44)$$

and

$$\mathbf{T} = -\frac{1}{4\pi} \mathbf{B} \otimes \mathbf{B} + \mathbf{g} \frac{B^2}{8\pi}. \quad (45)$$

Then we combine eq.(4), eq.(37), (40), and (43) into a closed system of equations very similar to nonrelativistic resistive MHD

$$\nabla \cdot \mathbf{B} = 0, \quad (46)$$

$$\frac{\partial \mathbf{B}}{\partial t} - \nabla \times (\mathbf{V} \times \mathbf{B}) - \eta \nabla^2 \mathbf{B} = 0. \quad (47)$$

$$\frac{\partial \rho}{\partial t} + \nabla \cdot (2\rho \mathbf{V}) = 0, \quad (48)$$

$$\frac{\partial \rho \mathbf{V}}{\partial t} + \nabla \left( -\frac{\mathbf{B} \otimes \mathbf{B}}{4\pi} + \mathbf{g} \frac{B^2}{8\pi} \right) = 0. \quad (49)$$

In these equations

$$\rho = e/c^2 = \frac{B^2}{8\pi c^2} \quad (50)$$

is the mass density of the electromagnetic field. There are however several differences. First, there is the factor of 2 in the second term of the “continuity equation” (48). Second, there is no  $\nabla(\rho\mathbf{V} \otimes \mathbf{V})$  term in the momentum equation. Finally, there is no “energy equation”. To some extent this similarity has been noticed in (Gruzinov 1999).

#### 4 THE INCOMPRESSIBLE LIMIT.

This system can be reduced even further if the equilibrium is supported predominantly by the magnetic pressure. Indeed, the dimensionless equations of momentum and continuity include small parameter  $\epsilon = \mu_c^2$

$$\epsilon \frac{\partial \rho \mathbf{V}}{\partial t} - \frac{1}{4\pi} (\mathbf{B} \cdot \nabla) \mathbf{B} + \nabla \frac{B^2}{8\pi} = 0. \quad (51)$$

$$\frac{\partial \rho}{\partial t} + 2\nabla(\rho \mathbf{V}) = 0, \quad (52)$$

Using the method of perturbation we expand the unknowns in powers of  $\epsilon$

$$\mathbf{B} = \mathbf{B}_0 + \epsilon \mathbf{B}_1, \quad \mathbf{V} = \mathbf{V}_0 + \epsilon \mathbf{V}_1, \quad \rho = \rho_0 + \epsilon \rho_1,$$

where

$$(\mathbf{B}_0 \cdot \nabla) \mathbf{B}_0 = 0. \quad (53)$$

To the zero order we have

$$\rho_0 = \frac{B_0^2}{8\pi c^2} = \text{const} \quad (54)$$

and

$$\nabla \cdot \mathbf{V}_0 = 0, \quad (55)$$

whereas the first order gives us

$$\rho_0 \frac{\partial \mathbf{V}_0}{\partial t} - \frac{1}{4\pi} (\mathbf{B}_1 \cdot \nabla \mathbf{B}_0 + \mathbf{B}_0 \cdot \nabla \mathbf{B}_1) + \nabla \frac{\mathbf{B}_1 \cdot \mathbf{B}_0}{4\pi} = 0. \quad (56)$$

This result shows us that eq.(51) differs from

$$\epsilon \rho \frac{\partial \mathbf{V}}{\partial t} - \frac{1}{4\pi} (\mathbf{B} \cdot \nabla) \mathbf{B} + \nabla \frac{B^2}{8\pi} = 0 \quad (57)$$

only by terms of order  $\epsilon^2$  and we may approximate equation (49) by

$$\rho \frac{\partial \mathbf{V}}{\partial t} - \frac{1}{4\pi} (\mathbf{B} \cdot \nabla) \mathbf{B} + \nabla \frac{B^2}{8\pi} = 0. \quad (58)$$

that implies the vorticity equation

$$\rho \frac{\partial \nabla \times \mathbf{V}}{\partial t} - \frac{1}{4\pi} \nabla \times (\mathbf{B} \cdot \nabla) \mathbf{B} = 0. \quad (59)$$

Thus, we have arrived to the following system of equations

$$\nabla \cdot \mathbf{B} = 0, \quad (60)$$

$$\nabla \cdot \mathbf{V} = 0, \quad (61)$$

$$\frac{\partial \mathbf{B}}{\partial t} - \nabla \times (\mathbf{V} \times \mathbf{B}) - \eta \nabla^2 \mathbf{B} = 0, \quad (62)$$

$$\rho \frac{\partial \nabla \times \mathbf{V}}{\partial t} - \frac{1}{4\pi} \nabla \times (\mathbf{B} \cdot \nabla) \mathbf{B} = 0. \quad (63)$$

This system of equations is very similar to the one of incompressible MHD. The only difference is that equation (58) involves the Eulerian time derivative whereas the vorticity equation of incompressible MHD involves the Lagrangian

time derivative (this, however, has no effect on the perturbation equations of the linear stability theory). One may argue that the limit of incompressible magnetodynamics is applicable only to a very limited range of problems as in general case the magnetic tension cannot be ignored and as the result one cannot assume that  $\rho$  is constant. We only point out that exactly the same argument applies to incompressible MHD unless the plasma magnetization is very low (Biskamp 1993).

Both in the nonrelativistic case (Priest & Forbes 2000) and in the case of magnetically dominated relativistic plasma (Lyutikov 2003) the most basic equilibrium current sheet configuration involves 1-dimensional current sheet with slab symmetry. Within this current sheet the magnetic field gradually rotates so that its pressure remains constant and its tension vanishes. Studying the stability of the relativistic current sheet Lyutikov(2003) derived the same growth rates for the tearing mode as in the nonrelativistic theory. Our analysis of the equations of resistive magnetodynamics explains this result as the direct consequence of the similarity between magnetodynamics and non-relativistic MHD. In the following section we study the tearing mode in some details.

#### 5 TEARING MODE INSTABILITY

Consider the stationary versions of eqs.(62,63)

$$\nabla \times (\mathbf{V} \times \mathbf{B}) - \eta \nabla^2 \mathbf{B} = 0, \quad (64)$$

$$\frac{1}{4\pi} \nabla \times (\mathbf{B} \cdot \nabla) \mathbf{B} = 0. \quad (65)$$

Low (1973) found the following one-dimensional solution for these equations

$$\mathbf{B} = B_0 \tanh(y/l) \mathbf{i}_x \pm B_0 \operatorname{sech}(y/l) \mathbf{i}_z, \quad (66)$$

$$\mathbf{V} = -(\eta/l) \tanh(y/l) \mathbf{i}_y. \quad (67)$$

It describes a current sheet in which the magnetic field rotates *exactly* by  $\pi$  without changing its magnitude. The rotation continues from  $y = -\infty$  to  $y = +\infty$  but most of it occurs within  $y \in [-l, l]$ . This allows us to describe  $l$  as the thickness of current sheet. The total electric field,  $\mathbf{E} = -\mathbf{V} \times \mathbf{B} + \eta \nabla \times \mathbf{B}$ , corresponding to this solution is

$$\mathbf{E} = -\frac{B_0 \eta}{l} \mathbf{i}_z. \quad (68)$$

It turns out that the electric and magnetic fields given by equations (67,68) also satisfy the full set of stationary Maxwell's equations supplemented with Ohm's law (13). (As a matter of fact this provides us with a very good test problem for our numerical code.)

Consider a perturbation of this equilibrium state of the form

$$\mathbf{b}(x, y, t) = \tilde{\mathbf{b}}(y) \exp(i(k_x x + k_y y) + wt),$$

$$\mathbf{v}(x, y, t) = \tilde{\mathbf{v}}(y) \exp(i(k_x x + k_y y) + wt).$$

Equation (62) and curl of equation (63) give us the following linearized equations for the the y-components of the perturbation

$$w\tilde{b}_y = i\tilde{v}_y(\mathbf{k} \cdot \mathbf{B}) + \eta(\tilde{b}_y'' - k^2\tilde{b}_y), \quad (69)$$

$$w(\tilde{v}_y'' - k^2\tilde{v}_y) = \frac{i(\mathbf{k} \cdot \mathbf{B})}{4\pi\rho} \left[ -\tilde{b}_y \frac{\mathbf{k} \cdot \mathbf{B}''}{\mathbf{k} \cdot \mathbf{B}} + (\tilde{b}_y'' - k^2\tilde{b}_y) \right]. \quad (70)$$

These equations are the same as equations 6.6 and 6.7 in Priest & Forbes (2000) where the tearing mode instability is studied in the non-relativistic framework of incompressible MHD (Priest & Forbes (2000) reproduced the original analysis by Furth et al.(1963) in a somewhat more concise and transparent way.) Thanks to this, the nonrelativistic theory and the relativistic theory should deliver exactly the same results. At this point we could simply refer the reader to the studies cited above but for the sake of completeness we briefly outline the analysis of Priest & Forbes (2000), clarifying few important issues along the way. Moreover, in our version we will use the steady state solution given by eqs.(67,67) instead of the step function

$$B_x = \begin{cases} +B_0 & \text{for } x > l, \\ B_0x & \text{for } |x| < l, \\ -B_0 & \text{for } x < -l. \end{cases}$$

used by the cited authors for the sake of simplicity.

Equation (70) is singular at the point where the wave vector is normal to the field direction in the equilibrium solution, that is where  $\mathbf{k} \cdot \mathbf{B} = 0$ . At this location there develops a thin *resistive sub-layer* where the second order derivatives become large just like in the classical boundary layer problem (e.g. Bush, 1992). With some loss of generality we will assume in what follows that  $k_z = 0$ , so that  $\mathbf{k} \cdot \mathbf{B} = kB_x$ . This puts the sub-layer right in the middle of the current sheet and makes the problem symmetric with respect to the plane  $y = 0$ .

Using  $l$  as a unit of length,  $\tau_d = l^2/\eta$  as a unit of time, and  $B_0$  as a unit of magnetic field strength we can write the dimensionless version of equations (69,70) as

$$\bar{w}\bar{b}_y = -\bar{v}_y f + (\bar{b}_y'' - \bar{k}^2\bar{b}_y), \quad (71)$$

$$\delta(\bar{v}_y'' - \bar{k}^2\bar{v}_y) = f \left[ -\bar{b}_y \frac{f''}{f} + (\bar{b}_y'' - \bar{k}^2\bar{b}_y) \right], \quad (72)$$

where

$$\bar{b} = \frac{\tilde{b}}{B_0}, \quad \bar{k} = kl, \quad \bar{w} = \frac{wl^2}{\eta}, \quad \bar{v}_y = -i\tilde{v}_y \frac{kl^2}{\eta},$$

$$f(\bar{y}) = \frac{B_x}{B_0} = \tanh \bar{y}, \quad \bar{y} = y/l,$$

and

$$\delta = \frac{\bar{w}}{L_u^2 \bar{k}^2} \ll 1$$

is a small parameter. Expanding  $\bar{b}_y$  and  $\bar{v}_y$  in powers of  $\delta$  we find the the leading terms satisfy

$$\bar{b}_y'' - \bar{k}^2\bar{b}_y + 2(1 - \tanh^2 \bar{y})\bar{b}_y = 0, \quad (73)$$

$$\bar{v}_y = \frac{\bar{b}_y}{\tanh \bar{y}}(2\tanh^2 \bar{y} - 2 - \bar{w}), \quad (74)$$

The solution to equation (73) that satisfies the boundary condition  $\bar{b}_y(+\infty) = 0$  is relatively simple

$$\bar{b}_y = \frac{b_0(\tanh \bar{y} + \bar{k})}{\bar{k}} \left( \frac{1 - \tanh \bar{y}}{1 + \tanh \bar{y}} \right)^{\bar{k}/2}. \quad (75)$$

Given  $\bar{b}_y$  one can find  $\bar{v}_y$  from eq.(71). Once  $b_y$  and  $v_y$  are known one can find  $b_x$  and  $v_x$  from the conditions

$$\nabla \cdot \mathbf{b} = 0, \quad \nabla \cdot \mathbf{v} = 0. \quad (76)$$

From eq.(75) we find that  $\bar{b}(0) = b_0$  and then eq.(71) shows that  $\bar{v}_y$  diverges at  $\bar{y} = 0$ . This indicates that around  $\bar{y} = 0$  there exists a sub-layer where the second order derivatives of  $\bar{v}_y$  in equation (69) become large and cannot be dropped. Thus, solution (75) applies only to the outside of this sub-layer and is called *the outer solution*. In fact, it holds only for  $\bar{y} > 0$ . The solution that applies for both sides of the sub-layer is

$$\bar{b}_y = \frac{b_0(\tanh |\bar{y}| + \bar{k})}{\bar{k}} \left( \frac{1 - \tanh |\bar{y}|}{1 + \tanh |\bar{y}|} \right)^{\bar{k}/2}. \quad (77)$$

This solution is continuous at  $y = 0$  but its first derivative changes sign at this point so that

$$\Delta' = \left[ \frac{\bar{b}_y'}{\bar{b}_y} \right]_{0-}^{0+} = 2 \frac{1 - \bar{k}^2}{\bar{k}} \quad (78)$$

These derivatives are to be used for matching the outer solution with *the inner solution* that describes the interior of the resistive sub-layer.

To find the structure of the resistive sub-layer, or the inner solution, we need to introduce new stretched variable  $\xi = \bar{y}/\delta^p$ , where the power of  $\delta$  is to be found using *the principle of least degeneracy* (Van Dyke 1975). Once  $p$  is known we will find thickness of the sub-layer as  $\epsilon = \delta^p$ . Here we may assume that inside the sublayer  $\bar{y} \ll 1$  and use the approximation  $f = \bar{y}$ . Combining equations (71) and (72) we find

$$\bar{b}_y = \frac{\delta}{\bar{w}} \frac{\bar{v}_y'' - \bar{k}^2\bar{v}_y}{\bar{y}} + \frac{\bar{y}}{\bar{w}} \bar{v}_y. \quad (79)$$

Substituting this result into eq.(71) we end up with a 4th order ODE for  $\bar{v}_y$ . When using the stretched variable this equation reads

$$\epsilon^2 \bar{v}^{(4)} - 2\bar{v}^{(3)} + \delta^{4p-1} \bar{v}^{(2)} + 2\delta^{4p-1} \bar{v}^{(1)} - \delta^{6p-1} \xi^4 (\bar{k}^2 + 2\bar{w}) v = A(\xi, v) \quad (80)$$

where  $A(\xi, v)$  includes all the term with positive power of  $\delta$ . One can see that when  $\bar{v}_y$  is expanded in powers of  $\delta$  the leading order equation will retain the largest number of terms if  $p = 1/4$ . Thus the dimensionless thickness of the sub-layer is

$$\epsilon = \left( \frac{\bar{w}}{L_u^2 \bar{k}^2} \right)^{1/4} \quad (81)$$

When using the stretch variable eq.(71) reads

$$\bar{b}_y^{(2)} - \epsilon^2 (\bar{k}^2 + \bar{w}) \bar{b}_y - \epsilon^3 \xi \bar{v}_y = 0. \quad (82)$$

To the second order in  $\epsilon$  we can ignore the last term in this equation and write

$$\bar{b}_y^{(2)} - \epsilon^2 (\bar{k}^2 + \bar{w}) \bar{b}_y = 0. \quad (83)$$

The solution of this equation that is symmetric with respect to the  $\xi \rightarrow -\xi$  transformation is

$$\bar{b}_y = b_0 \cosh(\sqrt{\bar{k}^2 + \bar{w}}\epsilon).$$

this gives us the jump in derivatives of  $\bar{b}_y$  across the sub-layer

$$\Delta' = \left[ \frac{\bar{b}_y'}{\bar{b}_y} \right]_{\bar{y}=-\epsilon}^{\bar{y}=\epsilon} = \frac{1}{\epsilon} \left[ \frac{\bar{b}_y^{(1)}}{\bar{b}_y} \right]_{\xi=-1}^{\xi=1} = 2(\bar{k}^2 + \bar{w})\epsilon. \quad (84)$$

Here  $\bar{b}_y'$  is the derivative with respect to  $\bar{y}$ .

Matching  $\Delta$ 's derived from the outer and the inner solutions, eq.(84) and eq.(78) respectively, allows us to find the growth rate for the mode with wavenumber  $\bar{k}$ :

$$(\bar{k}^2 + \bar{w}) \left( \frac{\bar{w}}{L_u^2 \bar{k}^2} \right)^{1/4} = \frac{1 - \bar{k}^2}{\bar{k}}. \quad (85)$$

One can see that only modes with wave numbers

$$\bar{k} < 1 \quad (86)$$

grow in amplitude. For  $\bar{k} \ll 1$  dispersion relation simplifies resulting in the well known equation

$$\bar{w} = \left( \frac{L_u}{k} \right)^{2/5}. \quad (87)$$

According to the last result the growth rate increases indefinitely with the wavelength. However, the e-folding time of the growing mode

$$\bar{\tau}_e = \frac{1}{\bar{w}} \quad (88)$$

cannot be shorter than the resistive time scale of the sub-layer

$$\bar{\tau}_e = \frac{\tau_e \eta}{l^2} = \epsilon^2. \quad (89)$$

This condition reads us

$$\bar{k} > \bar{k}^* = L_u^{-1/4}. \quad (90)$$

For smaller  $\bar{k}$  the growth is reduced and thus the maximum growth rate should be of order

$$\bar{w}^* = \bar{w}_{\bar{k}^*} = L_u^{1/2} \quad (91)$$

that corresponds to the dimensional time-scale

$$\tau^* = (\tau_e \tau_d)^{1/2}. \quad (92)$$

## 6 NUMERICAL METHOD

To verify the predictions of the theory of the tearing mode instability in relativistic magnetically dominated plasma we have carried out a series of numerical simulations. The equations that are solved numerically are the Maxwell equations (3-6) with the Ohm law

$$\mathbf{j} = \varrho \frac{\mathbf{E} \times \mathbf{B}}{B^2} c + \sigma_{\parallel} \mathbf{E}_{\parallel} + \sigma_{\perp} \mathbf{E}_{\perp}. \quad (93)$$

This differs from eq.(13) by the presence of the conductivity current across the magnetic field. However, we set  $\sigma_{\perp}$  to 0 when  $E^2 < B^2$  and thus eq.(93) reduces to eq.(13) during the linear and the beginning of the non-linear phases of the tearing instability. However, at some point of the non-linear phase a region develops where the electric field becomes stronger than the magnetic one thus allowing significant cross-field conductivity. We expect the particle pressure and inertia to become important in such regions resulting in a different form of the Ohm law. In fact, the MHD approximation may provide a more suitable mathematical framework there. However, in this study we are more focused on the linear theory and for this reason the prescription (93) suffice.

The numerical scheme used for simulations is a derivative of the general relativistic scheme for resistive magnetodynamics described in Komissarov (2004). Here, we give its brief description.

From eq.(3) one finds

$$\partial_t (\nabla \cdot \mathbf{B}) = 0. \quad (94)$$

This well known result shows that it is sufficient to enforce the divergence free condition (4) only for the initial solution and it will be satisfied automatically at any other  $t$ . Unfortunately, straightforward application of many numerical schemes perfectly suitable for other hyperbolic systems of conservation laws fails to deliver a good result for electrodynamics and MHD simply because their discrete equations are not consistent with any discrete analogue of (94). In particular, this applies to the method of Godunov which has many beneficial properties and is currently considered as generally superior to many other numerical schemes for hyperbolic systems. There have been many attempts to find a cure for this “div- $\mathbf{B}$  problem” ( see the review in Dedner et al., 2002.)

One of the ways to handle this problem involves construction of a somewhat different system of differential equations, the “augmented system”, where the divergence free condition (4) is no longer included and  $\nabla \cdot \mathbf{B}$  may be transported and/or dissipated like other dynamical variables. The idea is not to enforce the divergence free condition exactly but to promote a natural evolution of the system toward a divergence free state. Provided the augmented system is hyperbolic it can be solved numerically using the Godunov method (Munz 2000; Dedner et al. 2002).

Following this idea we modify eq.(3) as follows

$$\frac{1}{c} \frac{\partial \mathbf{B}}{\partial t} + \nabla \times \mathbf{E} + \nabla \Psi = 0 \quad (95)$$

where  $\Psi$  is the scalar field which is called the *pseudopotential*. Its evolution is given by

$$-\frac{1}{c} \frac{\partial \Psi}{\partial t} + \nabla \cdot \mathbf{B} + \kappa c \Psi = 0. \quad (96)$$

From these one finds that both  $\Psi$  and  $\nabla \cdot \mathbf{B}$  satisfy the telegraph equation

$$-\frac{1}{c^2} \frac{\partial^2 \Psi}{\partial t^2} + \kappa \frac{\partial \Psi}{\partial t} + \nabla^2 \Psi = 0. \quad (97)$$

$$-\frac{1}{c^2} \frac{\partial^2 \nabla \cdot \mathbf{B}}{\partial t^2} + \kappa \frac{\partial \nabla \cdot \mathbf{B}}{\partial t} + \nabla^2 (\nabla \cdot \mathbf{B}) = 0. \quad (98)$$

The resultant system includes two vector equations (95,5), and one scalar conservation law, equation (96). All these evolution equations can be written as conservation laws. In the form of an abstract vector equation they read

$$\frac{\partial \sqrt{\gamma} \mathcal{Q}}{\partial t} + \frac{\partial \sqrt{\gamma} \mathcal{F}^j}{\partial x^j} = \sqrt{\gamma} \mathcal{S}, \quad (99)$$

where

$$\mathcal{Q} = (\Psi, B^i, E^i) \quad (100)$$

are the conserved variables

$$\mathcal{F}^j = c (B^j, e^{ijk} E_k + \Psi g^{ij}, -e^{ijk} B_k) \quad (101)$$

are the corresponding hyperbolic fluxes,

$$\mathcal{S} = (\kappa c^2 \Psi, 0^i, 4\pi j^i). \quad (102)$$

In this study we employ Cartesian coordinates so that 1) the metric tensor of space  $g^{ij}$  equals to Kronecker's delta  $\delta^{ij}$ , 2) its determinant  $\gamma = 1$ , and 3) the Levi-Civita alternating tensor  $\epsilon^{ijk}$  reduces to the Levi-Civita symbol with  $\epsilon^{123} = 1$ .

Numerical integration of (99) is carried out using a second order Godunov method based in combination with the time-step splitting technique by Strang (1968) for handling the source term. Namely, each time-step  $t^n \rightarrow t^n + \Delta t$  is split into three sub-steps. During the first sub-step the numerical solution is advanced in time by  $\Delta t/2$  via integrating the truncated system

$$\frac{\partial \mathcal{Q}}{\partial t} = \mathcal{S}. \quad (103)$$

In fact we split the source term into two parts

$$\mathcal{S}_a = (\kappa c^2 \Psi, 0^i, 4\pi j_c^i) \quad \text{and} \quad \mathcal{S}_b = (0, 0^i, 4\pi j_d^i), \quad (104)$$

where  $j_c = \sigma_{\parallel} \mathbf{E}_{\parallel} + \sigma_{\perp} \mathbf{E}_{\perp}$  is the conductivity current and  $j_d = \varrho c \mathbf{E} \times \mathbf{B} / B^2$  is the drift current, and split this substep as well. First we account for  $\mathcal{S}_a$  only. This source term is potentially stiff but its simple form allows exact analytical integration of eq.(103) thus reducing the stability constraints on the timestep. Then we integrate eq.(103) with source term  $\mathcal{S}_b$  numerically using the method of Newton. During the second sub-step the resultant solution is advanced in time by  $\Delta t$  via integrating the truncated system

$$\frac{\partial \sqrt{\gamma} \mathcal{Q}}{\partial t} + \frac{\partial \sqrt{\gamma} \mathcal{F}^j}{\partial x^j} = 0 \quad (105)$$

using the second order Godunov scheme. The third sub-step is a repeat of the first one but now it is the solution found by the end of the second sub-step that is used as the initial solution for eq.(103).

In our Godunov scheme the numerical fluxes through the cell interfaces are found using the exact solution to the interface Riemann problems. The construction of this exact solver is simplified by the fact that system (105) is linear. Its 1D-version can be written as

$$\frac{\partial \mathcal{Q}}{\partial t} + \mathcal{A} \frac{\partial \mathcal{Q}}{\partial x} = 0 \quad (106)$$

with the Jacobean matrix

$$\mathcal{A} = c \begin{bmatrix} 0 & 1 & 0 & 0 & 0 & 0 & 0 \\ 1 & 0 & 0 & 0 & 0 & 0 & 0 \\ 0 & 0 & 0 & 0 & 0 & 0 & -1 \\ 0 & 0 & 0 & 0 & 0 & 1 & 0 \\ 0 & 0 & 0 & 0 & 0 & 0 & 0 \\ 0 & 0 & 0 & 1 & 0 & 0 & 0 \\ 0 & 0 & -1 & 0 & 0 & 0 & 0 \end{bmatrix}.$$

The eigenvalues of this matrix

$$\mu_{(1)} = \mu_{(2)} = \mu_{(3)} = c;$$

$$\mu_{(4)} = 0;$$

$$\mu_{(5)} = \mu_{(6)} = \mu_{(7)} = -c$$

provide the wavespeeds of hyperbolic waves. Other properties of these waves are given by the eigenvectors of  $\mathcal{A}$ . The right eigenvectors are

$$\begin{aligned} \mathbf{r}_{(1)} &= (1, 1, 0, 0, 0, 0, 0) \\ \mathbf{r}_{(2)} &= (0, 0, -1, 0, 0, 0, 1) \\ \mathbf{r}_{(3)} &= (0, 0, 0, 1, 0, 1, 0) \\ \mathbf{r}_{(4)} &= (0, 0, 0, 0, 1, 0, 0) \\ \mathbf{r}_{(5)} &= (-1, 1, 0, 0, 0, 0, 0) \\ \mathbf{r}_{(6)} &= (0, 0, 1, 0, 0, 0, 1) \\ \mathbf{r}_{(7)} &= (0, 0, 0, -1, 0, 1, 0) \end{aligned} \quad (107)$$

Since  $\mathcal{A}$  is symmetric its left eigenvectors,  $\mathbf{l}_{(i)}$ , coincide with the corresponding right eigenvectors:

$$\mathbf{l}_{(i)} = \mathbf{r}_{(i)}, \quad (108)$$

It is easy to see that solutions 2,3,6, and 7 are the usual electromagnetic waves. Solution 4 simply reflects the fact that all waves of vacuum electrodynamics are transverse and any discontinuity in the normal component of electric field is due to a surface electric charge distribution. Solutions 1 and 5 describe new waves that do not exist in electrodynamics; they transport  $\Psi$  and  $\nabla \cdot \mathbf{B}$ .

The solution to the Riemann problem with the left and the right states,  $\mathcal{Q}_{(l)}$  and  $\mathcal{Q}_{(r)}$ , and the interface speed  $\beta^x$  is

$$\mathcal{Q} = \mathcal{Q}_{(l)} + \sum_{i=1,3} \alpha_{(i)} \mathbf{r}_{(i)} \quad (109)$$

where the wave strengths

$$\alpha_{(i)} = \frac{(\mathcal{Q}_{(r)} - \mathcal{Q}_{(l)}) \cdot \mathbf{r}_{(i)}}{\mathbf{r}_{(i)} \cdot \mathbf{r}_{(i)}}.$$

Notice, that the 4th wave is ignored. The x-component of electric field is set to be the mean value of the left and the right states

$$E^x = 0.5(E_{(l)}^x + E_{(r)}^x). \quad (110)$$

The entire scheme is second order accurate in space and time provided  $\Delta t \leq \eta/c$ . The only stability constraint on the time step comes from the Currant condition  $\Delta t < \Delta x/c$  for eq.(105). However, the accuracy considerations may require a smaller time step. For example, our 1D test simulations of the equilibrium current sheet (67,67) have shown that if  $\Delta t = \eta/c$  then the relative error in  $E_z$  is around 10%.

## 7 COMPUTER SIMULATIONS

These are 2D simulations with slab symmetry in the z-direction (that is  $\partial f / \partial z = 0$  for any function  $f$ ). The utilized units are such that  $l = 0.1$ ,  $c = 1$ , and  $B_0 = 1$ . Following the setup of Sec.5 the initial equilibrium current sheet is normal to the y-axis and its symmetry plane is  $y = 0$ . The computational domain is  $[-x_0, +x_0] \times [-y_0, +y_0]$  with  $x_0 = \lambda/2$ , the half of the perturbation wavelength, and  $y_0 = 2.0$ . On the boundaries  $x = \pm x_0$  we impose the periodic boundary conditions and on the boundaries  $y = \pm y_0$  we impose the zero-gradient conditions. In order to get accurate solutions we have to have the resistive sub-layer well resolved. On the other hand, far away from the sub-layer the solution has no fine structure and does not require high resolution. This suggests to use a grid with variable resolution in the y-direction. We adopted the exponential rule

$$\Delta y_{i+1} = \begin{cases} \alpha \Delta y_i & \text{for } y_i < 0, \\ \alpha^{-1} \Delta y_i & \text{for } y_i > 0, \end{cases}$$

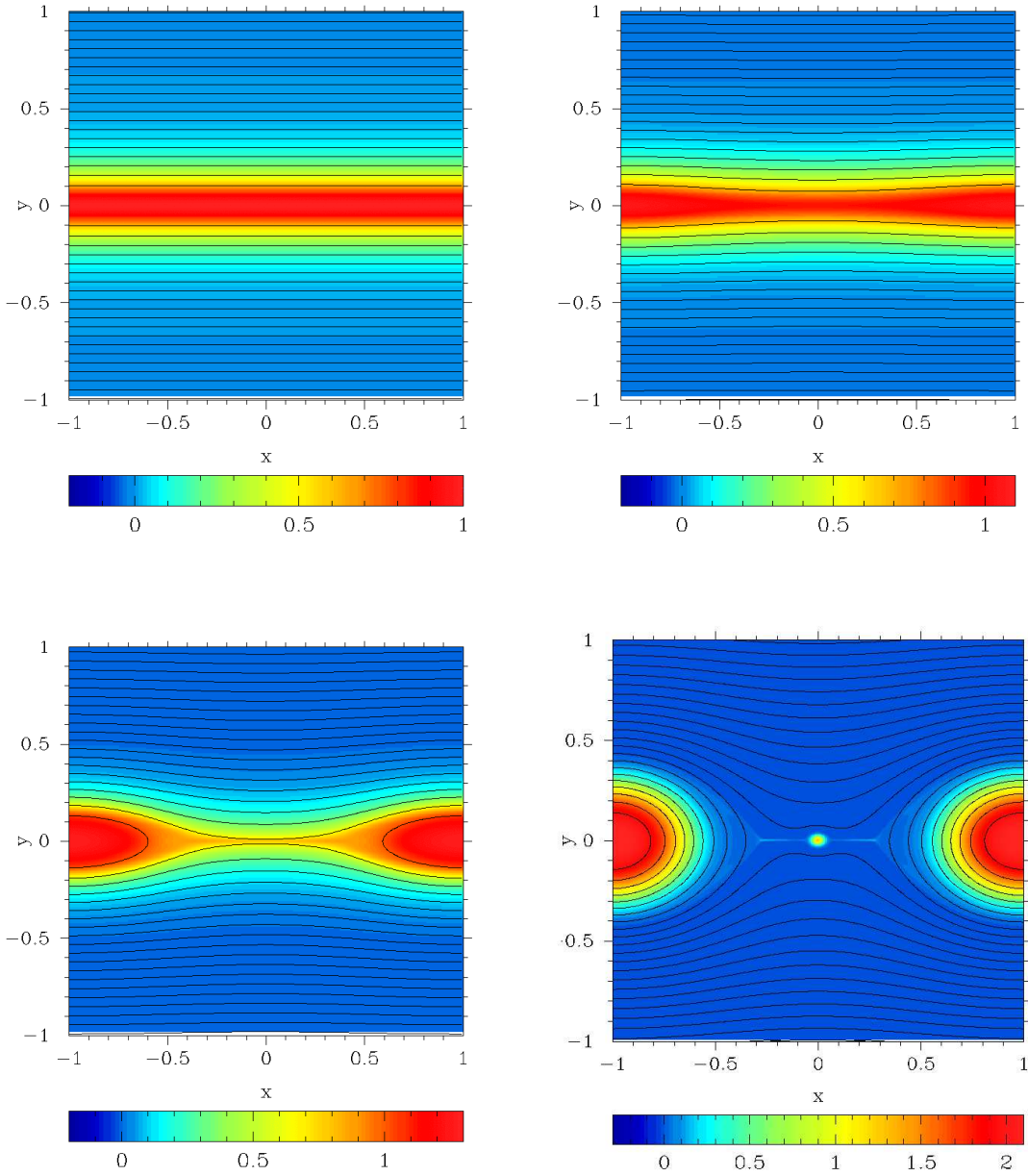


**Figure 1.** The evolution of the current sheet with  $\bar{k} = 0.314$  ( $\bar{k}L_u^{1/4} = 1.08$ ).  $B_z$  (color image) and the magnetic field lines at  $t = 0$  (top left),  $t = 5$  (top right),  $t = 10$  (bottom left), and  $t = 16$  (bottom right).

with the resolution in the symmetry plane being 10 times higher than that at the domain boundary,  $\Delta y(0) = 0.1\Delta y(y_0)$ . The resolution in the  $x$ -direction was uniform with  $\Delta x = \sqrt{0.1}\Delta y(y_0)$ .

We have tried two different models for the initial solution. In the first model the perturbation of the equilibrium solution (67,68) has the form

$$\mathbf{b} = (0, b_0 \sin(\pi x/x_0), 0), \quad \mathbf{e} = (0, 0, 0)$$

with  $b_0 = 10^{-3}$ . Since this is not the normal mode of the tearing instability the corresponding numerical solutions exhibited initial settling period of order  $\delta t \simeq 1$  before reaching the stage of exponential growth.

In the second model we tried to set up the normal mode.

In fact, we used the the outer solution (75,74) with  $b_0 = 10^{-3}$  in order to introduce the perturbation. Since, the electric field given by this solution diverges at  $y_0$  we resorted to linear interpolation in order to continue it within the resistive sub-layer. Perhaps this explains why the solution still exhibited approximately the same settling time as in first model. Moreover, we have not found any significant differences between the solutions corresponding to the both models except from their behavior during the settling.

We have considered only two values for the resistivity,  $\eta = 10^{-3}$   $\eta = 10^{-4}$ , corresponding to the Lundquist number  $L_u = 1.4 \times 10^2$  and  $L_u = 1.4 \times 10^3$  respectively. Figure 1 shows the evolution of the current sheet for  $\eta = 10^{-3}$  and  $\bar{k} = 0.314$ . As the perturbation grows the current sheet grad-

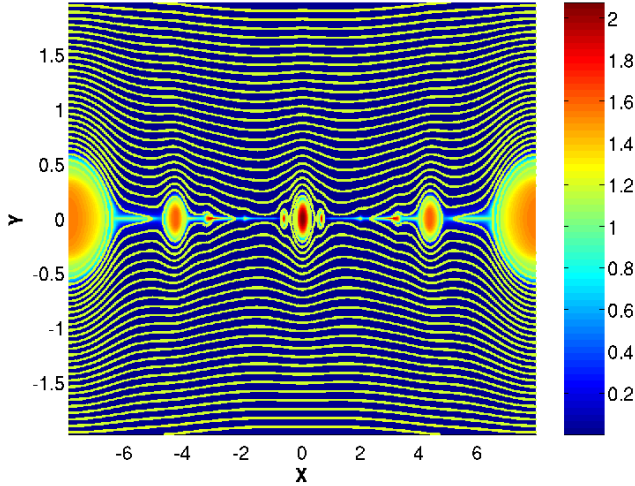


**Figure 2.** Multiple magnetic islands at the nonlinear stage of the model with  $\bar{k} = 0.0393$  ( $\bar{k}L_u^{1/4} = 0.135$ ,  $\eta = 10^{-3}$ ).

ually thins out in the middle of the domain and thickens at the x-boundaries. Eventually this results in the development of two large magnetic islands. By the end of the simulations a third much smaller island forms right in the middle. In fact, such secondary islands are typical and more pronounced for longer wavelengths. Figure 2 shows the final solution for the model with  $\bar{k} = 0.039$ . In this case there are free relatively large secondary islands and few smaller secondary islands in between them. These secondary islands originate in the following order. The larger secondaries develop when the two primaries suck in a large fraction of the current lines so that the residual current sheet becomes rather thin. These first secondary islands also suck in the current lines and this leads to further reduction of the thickness of the residual. Then new smaller islands appear between secondary island of the first generation and so on. This behavior seems to be caused by the reduction of the growth time for the tearing mode in thin current sheets.

As the thickness of the residual current sheet reduces,  $\nabla \times B$  goes up and so do the electric field and electric current density in the sheet. At some point the electric field, which is predominantly perpendicular to the magnetic field, reaches the same strength as the magnetic one and the drift speed reaches the speed of light. Eventually the current sheet collapses to the size of a computational cell and its electric field becomes even stronger than the magnetic field. This shows that the structure of the current sheet can no longer be described within our model and other factors like the thermodynamic pressure of plasma heated to high temperatures in the current sheet has to be taken into account. Prior to this point the quasi-equilibrium of the current sheet is basically supported by the magnetic pressure alone, the pressure of predominately x-directed magnetic field outside of the current sheet being balanced by the pressure of predominately z-directed magnetic field inside of it.

Figure 3 shows how the maximum value of  $B_y$  grows with time for different wavelengths of the perturbation in the case of  $\eta = 10^{-3}$ . One can clearly see that after the short initial settling period the growth of  $B_y$  becomes exponential. At this phase the primary islands dominate in the solution. This phase terminates when the nonlinear effects

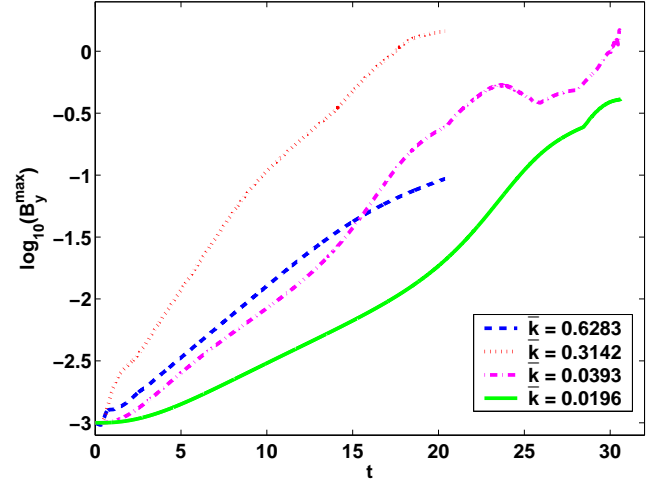


**Figure 3.** Growth of the perturbation for various wavenumbers ( $\eta = 10^{-3}$ ).  $B_y^{\max}$  is the maximum value of  $B_y$  on the grid.

become significant or when the smaller secondary islands overtake the primary ones (see the curves for  $\bar{k} = 0.0393$ , and  $0.0196$ ). There are two reasons for the faster growth of the secondary islands. Firstly, at the point of their appearance the thickness of the current sheet has been significantly reduced. Secondly, both the primary and the secondary islands correspond to wavenumbers  $\bar{k} < \bar{k}^*$ . In this regime (see figure 4) the perturbations of shorter wavelengths grow faster.

Figure 4 shows the dispersion relations  $\bar{w} = \bar{w}(\bar{k})$  that accounts for the growth rates of the primary islands. One can see that the dispersion curves have maximum at around  $\bar{k}^* = L_u^{-1/4}$  that agrees very well with the analytical results presented in Sec.5. The maximum growth rate is also close to the predicted  $\bar{w}_{\bar{k}^*} = L_u^{1/2}$ . Moreover, the results clearly indicated that modes with  $\bar{k} > \bar{k}_c = 1$  are indeed stable (see eq.85). The reason why the results for  $\eta = 10^{-4}$  give the maximum growth rate somewhat closer to the theoretical value than those for  $\eta = 10^{-3}$  may have to do with the fact that the separation between the cut-off wavenumber,  $\bar{k}_c$ , and  $\bar{k}^*$  becomes too short for relatively low Lundquist numbers.

## 8 APPLICATION TO MAGNETAR FLARES

One of the main unknowns in our calculations is the value of the resistivity  $\eta$ , which should be calculated from the particle kinetics, but instead was introduced as a macroscopic property of plasma - a common approach in continuous mechanics. Due to very short radiative decay times in magnetar magnetospheres the particles are bound to move only along the field lines, this limits considerably a number of possible resonant wave-particle interactions that can lead to development of plasma turbulence. The main remaining options are the Langmuir turbulence, which in relativistic plasma develops on a typical scale of electron skip depth,  $\delta_e \sim c/\omega_{p,e}$ , and ion sound turbulence, which in relativistic plasma develops on an ion skip depth  $\delta_i \sim c/\omega_{p,i}$  ( $\omega_{p,e}$  and  $\omega_{p,i}$  are the electron and ion plasma frequencies). They are different by a square root of the ratio of electron to ion masses  $\delta_e/\delta_i \sim (m_e/m_i)^{1/2}$ . A fully developed turbulence with a

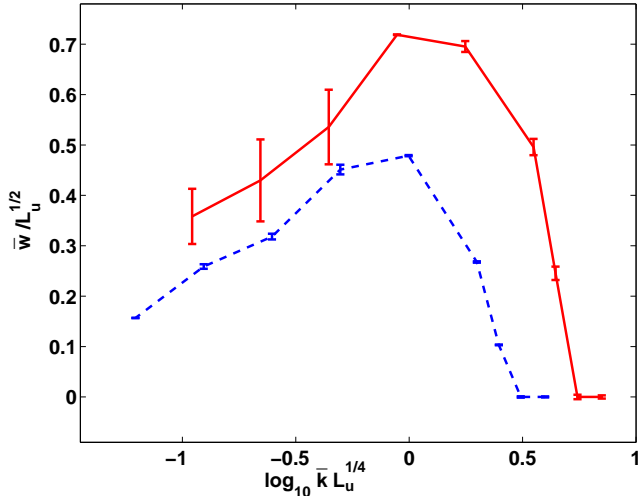


Figure 4. Growth rate as a function of the wavelength. Dashed line:  $\eta = 10^{-3}$  solid line:  $\eta = 10^{-4}$ .

typical velocity  $c$  and typical scale  $\delta$  would produce a resistivity  $\eta \sim c\delta$ . Thus we can write the growth time of tearing mode as

$$\tau \sim \frac{l}{c} \left( \frac{l}{\delta} \right)^{1/2} \quad (111)$$

Notice, that the result does not depend very much on which of the skin depths we use. The difference is in the factor  $(m_e/m_i)^{1/4} \simeq \text{few}$ . In current-carrying magnetospheres of magnetars the plasma frequency can be estimated as  $\omega_p = \lambda \sqrt{\omega_B r}/c$  ( $\lambda$  is a parametrization constant and  $r$  is the radial distance from the neutron star center) giving a growth time of the tearing mode

$$\tau = 2(B/B_Q)^{1/4} (l/R_{NS})^{7/4} \sqrt{\lambda} \text{ msec}, \quad (112)$$

where  $R_{NS}$  is the neutron star radius and  $B_Q$  is the quantum magnetic field. We also note that the expected Lundquist number is  $L_u \sim l/\delta \sim 5 \times 10^3 (B/B_Q)^{1/2} (l/R_{NS})^{3/2} \lambda^{-1/2}$ , which is close to the values used in our numerical simulations.

Although the connection between the growth time of the tearing mode and the observed flare rise time may not be that straightforward, the fact that the estimate (112) is close to a typical rise time of magnetar flares (Gögüs et al. 1999) is encouraging. Keeping in mind the uncertainties in the estimates of  $\eta$  and  $l$  we conclude that our model is consistent with observations.

## 9 CONCLUSIONS

The original idea of this study was to verify the surprising analytical results of (Lyutikov 2003) on the tearing instability in magnetically dominated relativistic plasma by means of direct numerical simulations. We have carried out such simulations and they fully confirmed Lyutikov's conclusion on the growth rate in magnetically dominated regime – it indeed coincides with that found earlier for the tearing instability in non-relativistic incompressible MHD, the shortest growth time being equal to the geometric mean of the Alfvén and resistive timescales (Furth et al. 1963;

Priest & Forbes 2000). Moreover, like in the non-relativistic case we observed formation of magnetic islands in the non-linear phase of the instability. This is accompanied by the appearance of noticeable O-type and X-type neutral points (or lines). The development of an X-point may be considered as a first step in setting up of reconnection layer where dissipated magnetic energy and magnetic flux are constantly replenished due to plasma inflow (Syrovatskii 1981).

Our results support the possibility of magnetar flares being magnetically driven reconnection-like events that occur in magnetar magnetospheres (Lyutikov 2003; Lyutikov 2006) in a similar fashion to flares and coronal mass ejections of Sun's magnetosphere. More complicated magnetic field geometries, e.g. those with nonvanishing magnetic tension, should also be subject to tearing instability on time scales intermediate between the resistive and Alfvén time scales (Priest & Forbes 2000). The growth rate typically scales as  $\tau \sim \tau_c^\alpha \tau_d^{1-\alpha}$ , where  $0 < \alpha < 1$  is some coefficient ( $\alpha = 1/2$  in our case). In the case of magnetar flares the observed flare rise-times range from fractions of a millisecond to  $\sim$  ten milliseconds, which is indeed intermediate between the Alfvén crossing time,  $\sim 0.03$  msec, and the resistive time,  $\sim$  seconds, of the magnetosphere (Lyutikov 2003).

The short timescale of tearing mode is achieved entirely through the formation of a very narrow resistive sub-layer with very short diffusion time scale. However, it is also expected that the resistivity itself may be enhanced inside such sub-layers due to the development of plasma turbulence (anomalous resistivity). Elucidating the properties of anomalous resistivity in such plasma is an important next step. Moreover, the collapse of current sheets and the eventual development in our simulations of the drift speeds exceeding the speed of light clearly indicates a breakdown of the MD approximation. In order to move forward one needs to put back the dynamical effects of matter which are bound to become important in this singular domain. The simplest way of doing this is to return to the model of relativistic MHD like in Lyutikov & Uzdensky (2003) and Lyubarsky (2005).

The coincidence of the growth rates for the tearing instability in incompressible MHD and MD clearly suggests some hidden similarity between the evolution equations of these two systems. We have carried out further analysis of resistive MD and discovered that in the quasi-equilibrium limit, that is characterized by low drift speeds, its equations do indeed become similar to those of non-relativistic MHD. In particular, the mass-energy density of the magnetic field takes on the role of the mass density of classic MHD whereas the drift velocity plays the role of the fluid velocity. *So the dynamics of the system can be described as a flow of magnetic mass-energy under the action of magnetic pressure and tension.* Moreover, the fact that the magnetic tension of the equilibrium current sheet subjected to tearing instability is zero allows further reduction of the MD equations which leads to almost the same system as incompressible MHD. When, this system is utilized in the analysis of the tearing instability it generates exactly the same equations for the perturbation as in incompressible MHD. Thus, our analysis provides perfect mathematical explanation for the surprising results in Lyutikov (2003) and improves our understanding of the dynamics of magnetically-dominated plasma.

Finally, we seem to have come up with a more suit-

able name for the system of equations describing the dynamics of relativistic magnetically dominated plasma. Instead of the currently used *force-free degenerate magnetohydrodynamics* (FFDE) or simply *force-free electrodynamics* (FFE) we propose to use *magnetodynamics* (MD). Let us summarize our arguments in favour of this new name. The current name originates from the early studies of stationary magnetospheres of neutron stars and black holes. Besides the steady-state Maxwell's equations, the key equations used in those studies were the degeneracy condition,  $\mathbf{E} \cdot \mathbf{B} = 0$ , and the condition of vanishing Lorentz force. The full system of the corresponding time-dependent equations was not known at the time and so were not known its connection with the relativistic MHD and the properties of its waves. All these have been discovered only very recently (Uchida 1997; Gruzinov 1999; Komissarov 2002). In Komissarov (2002) the dynamical equations of relativistic magnetically dominated plasma, equations (17-20), have been derived from the system of ideal relativistic MHD in the limit of vanishing rest mass density and pressure of matter. This way of derivation immediately suggests simply to remove the *hydro*-component from the word *magneto-hydro-dynamics*, which obviously results in the name we propose here. Like in ideal MHD, in ideal MD the electric field also vanishes in the the fluid frame, or to be more precise in the frame moving with the drift velocity. An inertial observer moving with this velocity would experience a pure magnetic field. Thus, it is desirable to retain the emphasis on the magnetic component of the electromagnetic field, that is present in the name of MHD. The key wave of MHD, the Alfvén wave, is also present in MD. It propagates along the magnetic field lines with the speed of light (Komissarov 2002). Like in MHD the electric field vector can be eliminated from the set of dependent variables of equations (17-20) (see Sec.2). Finally, as we have shown in this paper one can qualitatively describe the evolution of magnetically dominated plasma as a flow of magnetic energy under the action of Maxwell's stress. Apparently, we are not the only ones who are not particularly happy with the name force-free electrodynamics. Recently, A.Spitkovsky proposed to use the name *force-free MHD* instead (Spitkovsky 2006). This name is somewhat better but it is still not completely satisfactory. First of all, matter and the electromagnetic field appear in this name on equal terms, contrary to the relevant physical conditions. Secondly, the name MHD implies a somewhat different set of evolution equations. Thirdly, as we have seen, the resistive case can no longer be described as force-free. Finally, the name *magnetodynamics* is made of just one word that makes it more esthetically pleasing.

## ACKNOWLEDGMENTS

This research was funded by PPARC under the rolling grant "Theoretical Astrophysics in Leeds"

## REFERENCES

Aschwanden, M. J., 2002, Space Science Reviews, **101**, 1  
 Blandford, R.D., 2002. in Gilfanov M., Sunyaev, R., Churazov, E., (Eds.), *Lighthouses of the Universe*, Springer-Verlag, p.381.

Biskamp D., *Nonlinear Magnetohydrodynamics*, Cambridge Uni.Press, Cambridge, 1993.  
 Bush A.W., *Perturbation Methods for Engineers, Scientists*, CRC Press, Inc, Boca Raton, Florida, 1992.  
 Coroniti F. V., 1990, ApJ, **349**, 538.  
 Drenkhahn G., 2002, A&A, **387**, 714.  
 Drenkhahn G., Spruit H.C., 2002, A&A, **391**, 1141.  
 Dedner A., Kemm F., Kröner D., Munz C.-D., Schnitzer T., Weisenberg M., 2002, J.Comp.Phys, **175**, 645.  
 Furth H.P., Killeen J., Rosenbluth M.N., 1963, Phys.Fluids, **6**, 459.  
 Galeev, A. A., Coroniti, F. V., Ashour-Abdalla, M. , 1978, Geophys.Research Lett., **5**, 707  
 Priest E., Forbes T., *Magnetic Reconnection. MHD Theory , Applications*, Cambridge Uni.Press, Cambridge, 2000.  
 Göğüs E., Woods P.M., Kouveliotou C., van Paradijs J., Briggs M.S., Duncan R.C., Thompson C., 1999, ApJ.Lett, **526**, L93.  
 Gruzinov A., 1999, preprint, astro-ph/9902288.  
 Jaroschek C.H., Lesch H., Treumann R.A., 2004, ApJ.Lett., **605**, L9.  
 Kadomtsev, B.B., 1975, Soviet Journal of Plasma Physics, **1**, 710  
 Kennel, C.F. & Coroniti, F.V. 1984, ApJ, **283**, 710  
 Kirk J.G., Skjaraasen O., ApJ, **591**, 366.  
 Komissarov S.S., 1999, MNRAS, **303**, 343.  
 Komissarov S.S., 2002, MNRAS, **336**, 759.  
 Komissarov S.S., 2004, MNRAS, **350**, 427.  
 Low B.C., 1973, ApJ, **181**, 209.  
 Lyubarsky Y.E., 2006, MNRAS, **358**, 113.  
 Lyubarsky Y.E., Kirk J.G., 2001, ApJ, **547**, 437.  
 Lyutikov M., 2003, MNRAS, **346**, 540.  
 Lyutikov M., 2006, MNRAS, **367**, 1594  
 Lyutikov, M., & Uzdensky, D. 2003, ApJ, **589**, 893  
 Mereghetti, S. *et al* , 2005, ApJ, **628**,938  
 Munz C.-D., Omnes P., Schneider R., Sonnerdrücker, E., Voß U., 2000, J.Comp.Phys, **161**, 484.  
 Palmer, D. M. *et al* , 2005, Nature, **434**,1107.  
 Romanova M.M., Lovelace R.V.E., 1992, A&A, **262**, 26.  
 Rea, N., Tiengo, A., Mereghetti, S., Israel, G. L., Zane, S., Turolla, R., Stella, L., 2005, ApJ.Lett., **627**,133.  
 Shivamoggi, B. K., 1985, Astrophys.Sp.Sci., **114**, 15.  
 Spitkovsky A., 2006, astro-ph/0603147.  
 Strang G., 1968, SIAM J.Num.Anal., **5**, 506.  
 Syrovatskii S.I., 1981, Ann.Rev.Astron.Astrophys., **19**, 163.  
 Thompson C., Duncan R. C., 1995, MNRAS, **275**, 255.  
 Thompson, C., Lyutikov, M., Kulkarni, S. R., 2002, ApJ, **574**, 332  
 Thorne K.S., Macdonald D.A., 1982, MNRAS, **198**, 339.  
 Van Dyke M., *Perturbation Methods in Fluid Mechanics*, Parabolic Press, Palo Alto, CA, 1975.  
 Woods, P. M., Kouveliotou, C., Göğüs, E., Finger, M. H., Swank, J., Smith, D. A., Hurley, K., Thompson, C., 2001, ApJ, **552**, 748  
 Uchida T., 1997, Phys.Rev.E, **56**, 2181.  
 Usov V.V., 1994, MNRAS, **267**, 1035.